A quasi-elastic light scattering study of smooth muscle myosin in the presence of ATP

Xufeng Wu,* Paul S. Blank,‡ and Francis D. Carlson*

*Department of Biophysics, the Johns Hopkins University; ‡Division of Cardiology, the Johns Hopkins Medical Institutions, Baltimore, Maryland 21218 USA

ABSTRACT We have investigated the hydrodynamic properties of turkey gizzard smooth muscle myosin in solution using quasi-elastic light scattering (QELS). The effects of ionic strength (0.05–0.5 M KCl) and light chain phosphorylation on the conformational transition of myosin were examined in the presence of ATP at 20°C. Cumulant analysis and light scattering models were used to describe the myosin system in solution. A nonlinear least squares fitting procedure was used to determine the model that best fits the data. The conformational transition of the myosin monomer from a folded form to an extended form was clearly demonstrated in a salt concentration range of 0.15–0.3 M KCl. Light chain phosphorylation regulates the transition and promotes unfolding of the myosin. These results agree with the findings obtained using sedimentation velocity and electron microscopy (Onishi and Wakabayashi, 1982; Trybus et al., 1982; Trybus and Lowey, 1984). In addition, we present evidence for polymeric myosin coexisting with the two monomeric myosin species over a salt concentration range from 0.05 to 0.5 M KCl. The size of the polymeric myosin varied with salt concentration. This observation supports the hypothesis that, in solution, a dynamic equilibrium exists between the two conformations of myosin monomer and filaments.

INTRODUCTION

Studies on smooth muscle myosin over the past decade have established that the structure of this protein is significantly different from skeletal muscle myosin. There are two flexible joints in the smooth muscle myosin tail region, and only one flexible joint in skeletal myosin. This was shown by hydrodynamic and electron microscopy studies (Suzuki et al., 1978; Onishi and Wakabayashi, 1982; Trybus et al., 1982; Trybus and Lowey, 1984). The presence of two flexible joints allows an extended smooth muscle myosin (sedimentation coefficient 6S), which has the same structure as skeletal myosin, to fold its tail back on itself into three roughly equal sections, forming a folded configuration (sedimentation coefficient 10S). Recently, the folded (10S) form of myosin has also been found in the striated adductor muscle of the scallop, but there was no evidence for an unfolding transition involving the regulation of muscle contraction (Ankrett et al., 1991). However, the conformational transition of smooth muscle myosin from the extended form to the folded form may play an important role in regulating the slow and long lasting smooth muscle contraction. This folding–unfolding transition is regulated by solvent ionic strength and the state of phosphorylation of the regulatory light chain in the presence of MgATP. At ionic strengths above 0.3 M KCl, myosin reverts to the extended form, while at ionic strengths below 0.1 M KCl, myosin remains in the folded form. The transition between the two configurations of the myosin occurs in a narrow range of salt concentration from 0.175 to 0.225 M KCl where phosphorylation can shift the equilibrium in favor of the extended form (Trybus and Lowey, 1984).

The study of filament assembly in vitro has shown that the folded myosin monomers exhibit a very low critical monomer concentration (Kendrick-Jones et al., 1987) and when they lengthen into extended myosin by phosphorylation of the regulatory light chains, they can easily assemble into filaments at approximately physiological ionic strength (Craig et al., 1983; Kendrick-Jones et al., 1987). These observations support the hypothesis that a monomer–polymer equilibrium exists in smooth muscle cells in vivo with the special feature that the monomer can exist in two forms (Kendrick-Jones et al., 1987). Under physiological conditions (0.15 M NaCl, 1 mM MgATP, pH 7.0), the folded form remains soluble and is unable to form filaments. Light chain phosphorylation promotes the transition to the extended monomer and thus stimulates filament assembly. This regulated assembly of myosin from the soluble pool could be used as a means of fine adjustment of the force generating capacity of smooth muscle (Cross et al., 1988).

However, discrepancies in the monomer conformation have been found between the results obtained by sedimentation velocity and electron microscopy at a salt concentration range in which the myosin undergoes its conformational transition (Trybus and Lowey, 1984). These discrepancies could be due to perturbations introduced by the measurement technique. In electron microscopy studies, the conformation of myosin can readily change because of changes in salt and glycerol concentrations, and interaction between myosin and the mica substrate during sample preparation. In sedimentation velocity studies, the equilibrium state of the myosin system is disturbed by the centrifugal force field. In general, components of an equilibrium system form separate sedimenting boundaries that interfere with each other. Sometimes a large species is spun down rapidly and its boundary may not be seen when the boundaries of smaller species appear.

In this study, we have used the quasi-elastic light scat-

Address correspondence to Dr. Xufeng Wu.

0006-3495/92/07/169/11 $2.00

tering (QELS) technique to study the structural dynamics of smooth muscle myosin in solution at various ionic strengths and different phosphorylation states in the presence of MgATP. QELS is a technique based on measuring the fluctuations in the intensity of the light scattered from particles in solution without perturbing the system. The technique can provide a confirmation of previous studies and possibly a more accurate characterization of smooth muscle myosin in solution.

QELS has been used to determine the diffusion coefficients and the sizes of particles in solution for more than 20 yr (for reviews see Dahneke, 1983; Pecora, 1985). This method is powerful and well developed for the evaluation or interpretation of a monodisperse system containing spherical particles. However, most biological preparations are not monodisperse spherical particles and they require their own data analysis methods. These preparations can contain many components, some of which execute rotational motion, or internal motion by different parts of the molecules. Considerable effort has been devoted to expanding the capabilities of QELS for characterizing such samples and establishing its limitations.

The cumulant method (Koppel, 1972) was the first approach to determine the contributions of polydispersity to the autocorrelation function obtained by QELS measurements on a sample. The average decay rate and the width of the distribution of decay rates in the autocorrelation function can be accurately determined using the cumulant method. This method can give a rough measure of the sample polydispersity, but can not determine both the fraction and size of the particles in solution.

A variety of techniques for numerically inverting the autocorrelation function through the Laplace transformation have been developed to obtain not only the moments but the shape of the distribution of decay rates as well (Dahneke, 1983). If the scatterers are spherical, the decay rate for each scatterer is inversely related to the radius of the scatterer. Therefore, a simple transformation of the distribution of decay rates to the distribution of particle radii can be made. Specific computational schemes to accomplish the inverse Laplace transformation include Fourier expansion and eigenfunction expansion methods (Provencher, 1976a, b), a nonlinear least-square procedure (Provencher, 1978, 1979), and a least-square method using a histogram approximation (Chu et al., 1979). These schemes all require high quality data and considerable computation. They perform well only for a polydisperse solution containing spherical particles.

Although all the methods mentioned above have been applied with some success, analysis of polydispersity remains a major unsolved problem in this field. No general method exists to analyze QELS data for a polydisperse sample containing rod-like particles, such as smooth muscle myosin in solution. However, if the distribution of particle sizes obeys a particular functional form, the autocorrelation function can be analyzed directly to obtain parameters of the distribution. Since the autocorrelation function of a rigid rod can be expressed using an analytical form, it is possible to choose appropriate functional forms to model the polydisperse system under study. In this paper, we present models for a smooth muscle myosin system that have been developed from the published sedimentation velocity and electron microscopy studies (Onishi and Wakabayashi, 1982; Trybus et al., 1982) and used them to describe the conformational transition of smooth muscle myosin. A nonlinear least-squares algorithm was used to extract the smoothest, nonnegative distribution to the parameters of assumed models from the measured autocorrelation data. This data analysis procedure provides a means to study a polydisperse solution containing rod-like particles.

Our results for the myosin conformational transition are consistent with the findings obtained using sedimentation velocity and microscopy. In addition, we present evidence for polymeric myosin coexisting with the two forms of monomeric myosin in solution.

QELS MODELS FOR SMOOTH MUSCLE MYOSIN IN SOLUTION

The total intensity of light scattered from a collection of particles in solution will fluctuate as the positions and orientations of the particles change with time. Using the QELS technique, the dynamic properties of the particles can be studied by measuring the temporal fluctuations of the scattered light intensity. These fluctuations can be characterized quantitatively by the intensity autocorrelation function, $G^{(2)}(\tau)$, which is defined as:

$$G^{(2)}(\tau) = \langle I_s(t) I_s(t + \tau) \rangle, \quad (1)$$

where $I_s(t)$ is the instantaneous scattered light intensity, the angular brackets denote a time average over the duration of an experiment, and τ is a delay time. In the analysis of experimental data, it is more convenient to use the normalized optical field autocorrelation function,

$$g^{(1)}(\tau) = \langle E_s(t) E_s^*(t + \tau) \rangle / I_s(t), \quad (2)$$

where $E_s(t)$ is the scattered optical field. If the scattered field is Gaussian distributed with zero mean, which is the case for a solution of independent diffusing scatterers, $G^{(2)}(\tau)$ is related to $g^{(1)}(\tau)$, by the Siegert relationship (Mandel, 1963; Cummins, 1982):

$$G^{(2)}(\tau) = A(1 + \beta |g^{(1)}(\tau)|^2), \quad (3)$$

where A is a baseline constant, and β is an "instrument constant" arising primarily from the finite detector size. We can extract information about the dynamic properties of the particles, such as size, shape, and association by fitting $g^{(1)}(\tau)$ to a particular model.

Monomeric smooth muscle myosin can exist in two distinct conformations, an extended form with a length of ~160 nm and a folded form approximately one-third as long (Onishi and Wakabayashi, 1982). A transition from the extended form to the folded form occurs under certain physiological conditions. The molecule is assumed to behave hydrodynamically as a rigid rod in either conformation. If conformational change between the two forms is sufficiently rapid, a solution of pure monomeric smooth muscle myosin can then be modeled as a two component system of extended and folded rigid rods with weight fractions that vary with the ionic strength and phosphorylation state.

For the model system containing only two species, $g^{(1)}(\tau)$ can be expressed as:

$$g^{(1)}_{\text{total}}(\tau) = \sum_{i=1}^{2} f_{w,i} P_i(\theta) g_i^{(1)}(\tau, \theta) \Big/ \sum_{i=1}^{2} f_{w,i} P_i(\theta) \tag{4}$$

with

$$f_{w,1} + f_{w,2} = 1, \tag{5}$$

where $f_{w,i}$ is the weight fraction for the ith species, $P_i(\theta)$ is the form factor for the ith species, and $g_i^{(1)}(\tau, \theta)$ is the field autocorrelation function for the ith species. $P_i(\theta)$ represents the modification of the intensity due to the finite size of the particle and its deviation from sphericity.

If the length, L, of a rod-like particle is comparable to the wavelength, then its light scattering characteristics are different when observed at different scattering angles. The scattering vector, $\vec{q}$, defined as the difference between the scattered and incident wave vectors, is the key experimental variable in probing the diffusive motions of a particle. The magnitude of $\vec{q}$ is given by:

$$q = |\vec{q}| = \frac{4\pi n}{\lambda_0} \sin\left(\frac{\theta}{2}\right), \tag{6}$$

where λ_0 is the wavelength of light, θ the scattering angle, and n the refractive index. Two models were used in this work to characterize the scattering dynamics of smooth muscle myosin over different ranges of qL and they are described as follows.

(a) Two sphere model

For small scattering angles where $qL < 3$, the rotational motion of the species is not observable and a rod-like particle appears as a sphere in a QELS measurement. The values of qL are 1.5 and 0.5 for extended and folded myosins with lengths of 150 and 50 nm, respectively, using 488 nm incident light at a 30° scattering angle. Under this condition, myosin monomers are just small enough to justify neglecting rotational diffusion effect in the analysis. The system, therefore, can be described by a two sphere model, in which the two myosin monomers diffuse like two differently sized spheres in solution. The field autocorrelation function for each molecule can be expressed as a single exponential with a form factor close to unity. Therefore, the autocorrelation function for this system, reduces to:

$$g^{(1)}_{\text{total}}(\tau) = f_{w_1} e^{-\Gamma_1 \tau} + f_{w_2} e^{-\Gamma_2 \tau} \tag{7}$$

$$\Gamma_1 = D_{T_1} q^2 \tag{8}$$

$$\Gamma_2 = D_{T_2} q^2, \tag{9}$$

where Γ_1 and Γ_2 are the decay rates of the field autocorrelation function, and D_{T_1} and D_{T_2} are the translational diffusion coefficients, for the first and second species, respectively.

(b) Two cylinder model

For large scattering angles where $qL > 3$, the rotational motion cannot be ignored, and the particle no longer approximates a sphere. The values of qL for both myosin monomeric species are greater than 3 but less than 10 for scattering angles between 50° and 150°. Under these conditions, a monomeric myosin solution can be described by a two cylinder model, in which the two conformationally different myosin monomers diffuse as two kinds of cylinders in solution.

For $3 < qL < 10$, the field autocorrelation for each molecule, $g^{(1)}(\tau, \theta)$, is well approximated by the first two terms of an infinite series (Cummins, 1982):

$$g_i^{(1)}(\tau, \theta) = \frac{1}{P_i(qL)} \times \{B_0 e^{-D_T(L_i, r_i) q^2 \tau} + B_2 e^{-[D_T(L_i, r_i) q^2 + 6 D_R(L_i, r_i)]\tau}\}, \tag{10}$$

where $B_h = (2h + 1)[(2/qL) \int_0^{qL/2} j_h(x) dx]^2$ with $h = 0, 2$, D_T and D_R are the translational and rotational diffusion coefficients, and $j_h(x)$ is the spherical Bessel function of order h. For a thin cylindrical particle, the form factor in Eq. 4 is a function of qL and is given by the Rayleigh-Debye approximation (Kerker, 1969):

$$P(qL) = \frac{2}{qL} \int_0^{qL} \frac{\sin(x)}{x} dx - \left[\frac{\sin(qL/2)}{qL/2}\right]^2. \tag{11}$$

The translational and rotational diffusion coefficients, D_T and D_R, in Eqs. 8, 9, and 10, were calculated using Broersma's relations (Broersma, 1960a, b, 1981) for a rigid rod of length L and radius r:

$$D_T = \frac{kT}{3\pi\eta L}\left[\delta - \frac{1}{2}(\gamma_{\parallel} + \gamma_{\perp})\right] \tag{12}$$

$$D_R = \frac{3kT}{\pi\eta L^3}(\delta - \zeta), \tag{13}$$

where $\delta = \ln(L/r)$, $\gamma_{\parallel} = 1.27 - 7.4(1/\delta - 0.34)^2$, $\gamma_{\perp} = 0.19 - 4.2(1/\delta - 0.39)^2$, $\zeta = 1.45 - 7.5(1/\delta - 0.27)^2$, and η is the viscosity of the solvent.

METHODS

Preparation of proteins

Turkey gizzard myosin was prepared as described by Sellers (Sellers et al., 1981) with some modifications in the purification step. The crude myosin was first dialyzed through two cycles of a salt-in and salt-out procedure in order to remove actin. The myosin was allowed to precipitate by dialysis against 2 liters of a low salt buffer (20 mM KCl, 2.5 mM K_2HPO_4, 2.5 mM KH_2PO_4, 1 mM EGTA, 0.5 mM DTT, 1 mM NaN_3, 20 mM $MgCl_2$, pH 6.5) for 18 h with a solution change every 6 h. For the first 6 h of dialysis the buffer contained no $MgCl_2$. Myosin will precipitate, while actin and tropomyosin remain soluble. After dialysis the myosin was collected by centrifugation at 30,000 *g* for 30 min. The myosin pellet was then redissolved in a minimum volume of high salt buffer (0.6 M KCl, 10 mM K_2HPO_4, 10 mM KH_2PO_4, 2 mM EGTA, 2 mM DTT, 2 mM NaN_3, pH 7.5) and dialyzed against the same buffer overnight. The myosin was then clarified in the centrifuge at 29,000 *g* for 1 h. The myosin was further purified by gel filtration on a 2.5 × 88 cm Sephacryl S-400 column equilibrated and eluted with buffer (0.6 M NaCl, 20 mM N_2HPO_4, 1 mM EDTA, 0.5 mM DTT, and 2 mM NaN_3, pH 7.0). The myosin peak was identified by its absorbance at 280 nm using a spectrophotometer and confirmed by SDS-polyacrylamide gel electrophoresis. Myosin prepared in this way was free from actin as determined by 8.5% SDS-gel electrophoresis and was more than 90% unphosphorylated according to Trybus and Lowey (1984). Myosin concentration was determined by using the extinction coefficient $\epsilon_{280}^{1\%} = 5.0$ (Trybus and Lowey, 1984). The column purified myosin was stored at 0°C and used within a week after purification.

Phosphorylated turkey gizzard myosin was provided by Dr. James R. Sellers from the laboratory of Molecular Cardiology (National Heart, Lung, and Blood Institute, NIH) and was prepared as described by Sellers et al. (1981). The sample was fully phosphorylated and column purified by using Sepharose 4B (Sellers et al., 1981). It was stored at 0°C and used within a week.

Preparation of samples

Phosphorylated and unphosphorylated myosin were diluted into and dialyzed against buffers having the desired ionic conditions. Buffers were prepared by adding different amounts of KCl to the solvent containing 5 mM K_2HPO_4, 5 mM KH_2PO_4, 5 mM $MgCl_2$, 1 mM EGTA, 1 mM DTT. Concentrations of KCl in the solutions varied from 0.05 to 0.5 M. The pH value of each solution was adjusted to 7.5 using KOH. The protein concentrations for QELS measurements were ~0.1 mg/ml. Before the QELS measurements, 1 mM MgATP was added to the sample in order to dissociate polymeric forms of myosin, and then centrifuged at 100,000 *g* for 45 min at 4°C. The middle third of the supernatant in the centrifuge tube was transferred to an acetone-washed cuvette using a prewashed 0.22-μm filter. The sample cuvette was a standard 1 × 1 × 2 cm or 1 × 1 × 3 cm stopped cuvette of fused silica (Hellma OS 101; Hellma Cell Inc., Forest Hills, NY). The sample transfer was done in a positive pressure dust-free glove box to avoid dust contamination. The sample cuvette was precleaned following the procedure described by Montague and Carlson (Montague and Carlson, 1982). After the clean cuvette was filled, it was placed in a swinging bucket rotor and centrifuged at 1,000 *g* for 10 min to further reduce dust contamination. Before collecting data, samples were placed in the spectrometer to check for the presence of dust. The sample was rejected if a significant amount of dust was present, as indicated by visible bright transient flashes of scattered light in the forward direction just off the main laser beam or by large erratic fluctuations in the count rate. In the experiments, three procedures were taken to insure that no impurities existed in samples: (*a*) the preparation was clarified at 100,000 *g* for 45 min to 3 h; (*b*) the low speed spin at 1,000 *g* was performed on the same sample between two subsequent measurements; and (*c*) a repeated measurement was made on each sample after storage at 4°C over night. No significant difference in sample polydispersity was observed following each of these procedures. All the experiments were conducted at 20°C.

QELS spectrometer

The light scattering spectrometer was built in this laboratory (Newman and Carlson, 1980). The source of light was a Lexel model 95-2 Argon laser (Lexel Corp., Fremont, CA) operating in a single mode at a wavelength of 488 nm. The intensity fluctuation of the laser was less than ±0.2% over twelve operating hours using the light regulation mode. The waist of the laser beam was ~100 μm at the center of the sample cell. The scattered light was collected by a photomultiplier (model FW4085; ITT, Fort Wayne, IN), and the output pulses processed by an amplifier (model 133B; LeCroy Research System Co., Spring Valley, NY) and a discriminator (model T101/N; ORTEC Inc., Oak Ridge, TN).

Data collection

Data were collected with a real-time correlator (model 1096; Langley Ford Instruments, Amherst, MA) which directly computes the intensity correlation function, $G^{(2)}(\tau)$. For each experimental run, $G^{(2)}(\tau)$ was transferred to a computer (UNIXPC 3B1; AT&T, Iselin, NJ) from the correlator for off-line analysis. The protocol for collecting QELS data from each sample was as follows. In a typical experiment, seven sets of data were collected from a single protein sample. A set of data consisted of the data collected at each of seven scattering angles spaced at 20° intervals between 30°–150°. A group of 10 consecutive 'mini experiments' was performed at each scattering angle. Each 'mini-experiment' in a set was a single measurement of $G^{(2)}(\tau)$ using the identical sample time, $\Delta\tau$, and for the same experimental duration time, T. The sample time is related to the delay time by $\tau = m\Delta\tau$, where m is the channel number. It was selected so that the entire correlation duration spanned ~2–3 coherence times, t_c (Oliver, 1974). The background counts, A, for each mini-autocorrelation function was taken as the average value of the data stored in the last 16 channels in the correlator, which were delayed by 1,024 sample times. The experimental duration time was chosen so that the background counts were at least 1×10^5 for a mini-measurement. Each mini-observation of $G^{(2)}(\tau)$ was normalized by its own measured background in the data analysis procedure.

Data analysis

The intensity autocorrelation function, $G^{(2)}(\tau)$, obtained from the correlator was analyzed using two methods: the cumulants method (Koppel, 1972), and the model fitting method. The former was performed on $G^{(2)}(\tau)$ for an initial estimate of sample monodispersity. The later was then performed on the normalized field autocorrelation function, $g^{(1)}(\tau)$, to obtain more precise information about the sample.

Cumulant analysis

The method of cumulants is a standard method used for detecting the presence of polydispersity in a sample. This method estimates the moments of the distribution of decay rates in the autocorrelation function. The first moment represents the average decay rate, $\bar{\Gamma}$, and the second moment is the width of the distribution of the decay rates, μ_2. They are related to the dynamic properties of the sample by:

$$\bar{\Gamma} = \overline{D_{\text{eff}}}\, q^2 \tag{14}$$

$$\mu_2 = \overline{(\Gamma - \bar{\Gamma})^2} = \overline{[(D_{\text{eff}} - \overline{D_{\text{eff}}})^2]}\, q^4, \tag{15}$$

where $\overline{D_{\text{eff}}}$ is a weighted, average, effective diffusion coefficient of the sample.

This method can be used to detect the departure of the autocorrelation function from a single exponential form as occurs with polydisperse and/or nonspherical particles. The polydispersity index, Q, which gives a measure of this departure, is defined as:

$$Q = \frac{\mu_2}{\bar{\Gamma}^2} = \frac{\overline{(D_{\text{eff}} - \overline{D_{\text{eff}}})^2}}{\overline{D_{\text{eff}}^2}} = \frac{\overline{\Delta D_{\text{eff}}^2}}{\overline{D_{\text{eff}}^2}}. \tag{16}$$

Usually a value of $Q \leq 0.05$ indicates a monodisperse suspension of spherical or point scatterers. For a monodisperse sample of rigid rods,

Q is a measure of the asymmetry of the particle. The longer the rod is, the higher the value of Q. However, a sufficiently short rod behaves like a spherical particle when $qL < 3$. In this case, the value of Q is a measure of polydispersity of the sample containing rod-like particles. The cumulant method can give a rough measure of sample polydispersity, but cannot be used to determine the fraction and size of different species in solution.

Model fitting

In model fitting, the Levenberg-Marquardt algorithm (Levenberg, 1944 and Marquardt, 1963) was employed for the nonlinear least squares fitting routine. The goodness of fit to the experimental $g^{(1)}(\tau)$ was examined by calculating the chi-square per degree of freedom, χ_ν^2, (Bevington, 1969):

$$\chi_\nu^2 = \frac{\chi^2}{N - n}, \qquad (17)$$

where N is a number of data points and n is the number of fitting parameters. If the assumed model is a good approximation to the data, the value of χ_ν^2 should be approximately one.

Data collected at the 30° scattering angle was analyzed using the two sphere model. The fitting parameters were the weight fraction for one of the species and the translational diffusion coefficients for both species. Data collected at the 90° scattering angle was analyzed using the two cylinder model. To simplify the data analysis and improve the accuracy of the fitting parameters, the dimensions of one of the cylinders, which represented either the folded or the extended myosin in the model, were specified based on the results obtained from the two spheres model fitting and the previous results obtained from electron microscopy (Onishi and Wakabayashi, 1982). The fitting parameters for the two cylinder model became the weight fraction of the specified species, the length, and radius of the other species.

RESULTS

Cumulant analysis

Average decay rate

The two forms of smooth muscle myosin were examined in high salt (0.3 M KCl) and low salt (0.1 M KCl) concentrations at scattering angles ranging from 30° to 150°. The average decay rates, $\bar{\Gamma}$, of the autocorrelation function as a function of the square of the scattering vector, q^2, are presented in Fig. 1 for phosphorylated and unphosphorylated myosin.

Theoretical estimations of $\bar{\Gamma}$ are also plotted in Fig. 1 for the two forms of myosin, assuming a length of 150 nm and a radius of 1 nm for the extended form, and a length of 50 nm and a radius of 3 nm for the folded form. For both phosphorylated and unphosphorylated myosin, samples at the high salt concentrations exhibit slow decay rates consistent with the theoretical estimates for an extended form. At the low salt concentrations, samples exhibit high decay rates consistent with the theoretical estimates for a folded form. These results demonstrate the presence of two salt dependent conformational components in smooth muscle myosin solutions in both phosphorylation states. The sizes of these two components are consistent with the published values (Onishi and Wakabayashi, 1982; Trybus et al., 1982).

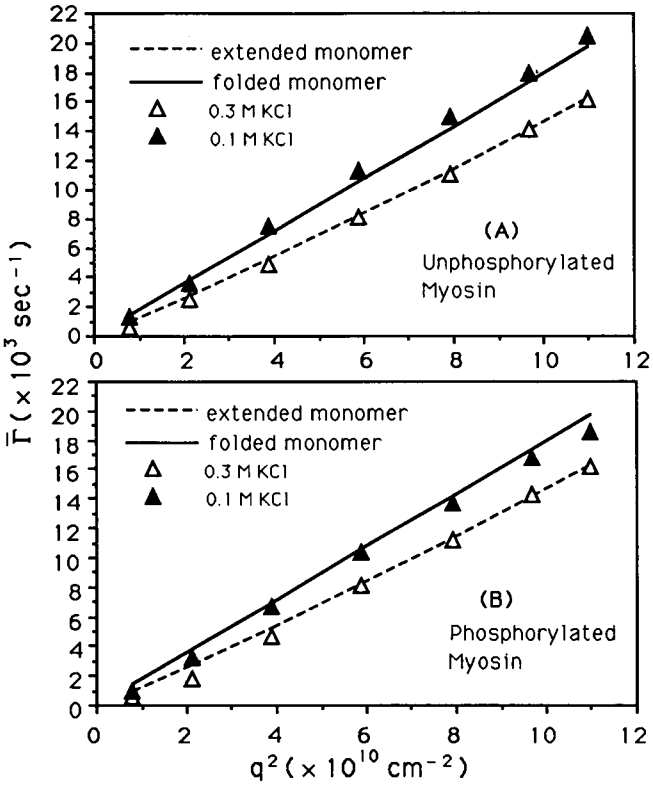

FIGURE 1 Average decay rate, $\bar{\Gamma}$, of a smooth muscle myosin solution as a function of the square of the scattering vector, q^2. $\bar{\Gamma}$ was obtained using the cumulant method for unphosphorylated (*A*) and phosphorylated (*B*) myosin. The myosin samples were dialyzed against KCl concentrations of 0.3 M (*open symbols*) and 0.15 M (*filled symbols*) with a buffer of 5 mM K_2HPO_4, 5 mM KH_2PO_4, 5 mM $MgCl_2$, 1 mM EGTA, and 1 mM DTT, pH 7.5. The protein concentration was 0.11 ± 0.02 mg/ml. The experiments were conducted at 20°C and 1 mM MgATP was added before the measurements. The error in each point is the same as or smaller than the size of the symbols on the plot. The theoretical decay rates for a folded myosin (50 nm in length and 3 nm in radius) and an extended myosin (150 nm in length and 1 nm in radius) are presented as solid and dashed lines, respectively.

Effective diffusion coefficients

The conformational transition between the two forms of myosin were studied by dialyzing the sample into different salt concentrations between 0.05 and 0.5 M KCl. Autocorrelation functions of the phosphorylated and unphosphorylated myosin were measured as a function of salt concentration at scattering angles ranging from 30° to 150°. As was found for the data shown in Fig. 1, the dependence of the $\bar{\Gamma}$ on q^2 was roughly linear at the different salt concentrations. The slope of the best-fit straight line gives the weighted, average, effective diffusion coefficient, $\overline{D_{\text{eff}}} = \bar{\Gamma}/q^2$, of the sample. A plot of the ionic strength dependence of $\overline{D_{\text{eff}}}$ is shown in Fig. 2. The experimental data were fit with a two-state model for phosphorylated and unphosphorylated myosin (*solid line* in Fig. 2), assuming all myosin species were in either a folded state at low ionic strength or an extended state at high ionic strength.

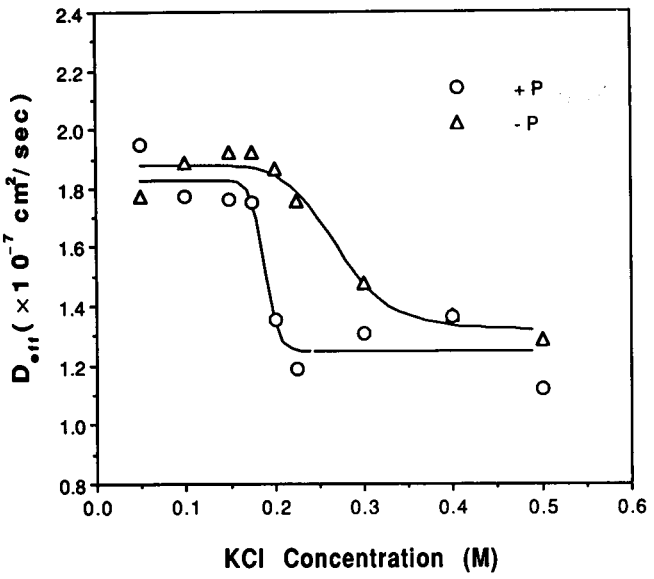

FIGURE 2 Effective diffusion coefficients, $\overline{D_{eff}}$, of myosin as a function of salt concentration. $\overline{D_{eff}}$ for phosphorylated (○) and unphosphorylated (△) myosin was obtained from the slope of the best-fitted curve of $\bar{\Gamma}$ vs. q^2 at KCl concentration of 0.050 M, 0.100 M, 0.150 M, 0.175 M, 0.200 M, 0.225 M, 0.300 M, 0.400 M, and 0.500 M with a buffer of 5 mM K_2HPO_4, 5 mM KH_2PO_4, 5 mM $MgCl_2$, 1 mM EGTA, 1 mM DTT, and 1 mM MgATP (pH 7.5). The protein concentration was 0.11 ± 0.02 mg/ml. The experiments were conducted at 20°C. The solid lines are fitted curves of phosphorylated and unphosphorylated myosin assuming a two state conformational transition from a folded form to an extended form. The error in each point is the same as or smaller than the size of the symbols on the plot.

Fig. 2 shows that there are two distinguishable diffusing species in both unphosphorylated and phosphorylated myosin at the two extremes of KCl concentrations. Effective diffusion coefficients of the myosin at low salt concentrations (≤0.15 M KCl) were nearly 1.5 times as large as those at high salt concentrations (≥0.30 M KCl). In low salt, the $\overline{D_{eff}}$ values were 1.8×10^{-7} to 1.9×10^{-7} cm^2/s, corresponding to an effective hydrodynamic radius of 11.3 to 11.9 nm. In high salt, the values of $\overline{D_{eff}}$ were 1.25×10^{-7} cm^2/s to 1.35×10^{-7} cm^2/s, corresponding to an effective hydrodynamic radius of 15.9 to 17.1 nm. These values are consistent with the values of the Stokes radius for the 10S form (folded) and the 6S form (extended) obtained from sedimentation velocity experiments (Trybus et al., 1982). If the species are modeled as rigid rods with a 1 or 3 nm radius, the length of the slower diffusing component is 145 to 150 nm, and the length of the faster diffusing component is 45 to 50 nm. These values agree with the expected values for the extended and folded forms.

The transition from a faster diffusing species to a slower diffusing species took place at an intermediate range of KCl concentrations, 0.15 to 0.30 M KCl, where the effective diffusion coefficients were strongly dependent on phosphorylation of the myosin light chain. As shown in Fig. 2, unfolding occurred at a lower KCl concentration for phosphorylated myosin than it did for unphosphorylated myosin. In other words, phosphorylation favored the extended state of myosin. The salt dependence of the conformational transition was different for phosphorylated and unphosphorylated myosin. $\overline{D_{eff}}$ values of unphosphorylated myosin decreased more slowly with increasing salt concentration than it did for phosphorylated myosin. These observations agree with the results obtained from sedimentation velocity experiments (Trybus and Lowey, 1984).

Polydispersity

The polydispersity index Q, is a measure of the departure of a system from a monodisperse solution of spheres. A polydisperse solution or a solution of asymmetric particles exhibits a high value of Q. In practice, the Q value measured from 0.1 μm diameter polystyrene latex spheres is less than 0.05. In general, $Q > 0.05$ is found for a non-monomeric solution or a solution containing a single asymmetric species. The Q values of the unphosphorylated and phosphorylated myosin varied from 0.12 to 0.6, depending on the salt concentration and scattering angle. The highest values were obtained at forward scattering angles ($\theta < 50°$) for a given sample. At 30° scattering angle, the value of Q increased from 0.2 to 0.6 as the KCl concentration in the sample solution increased from 0.05 to 0.5 M. At 150° scattering angle, the value of Q increased from 0.12 to 0.36 as the KCl concentration increased over the same range. If myosin existed only in a completely folded or completely extended form, a much smaller Q would have been obtained. The high values of Q found at forward scattering angles are consistent with a polymeric myosin solution, because particle asymmetry effects are negligible in the forward scattering direction. The high values of Q found for forward scattering and the low values found for backward scattering could be due to some large species in solution. Such a large species would contribute less scattered light in the backward direction, and cause Q to decrease as the scattering angle increases. For backward scattering, the higher values of Q for high salt concentrations suggest the presence of a highly asymmetric particle. Thus, the average length of rodlike particles must have been greater in high salt solutions than in low salt solutions. There appeared to be a multispecies equilibrium in the myosin solution. However, the cumulant method lacks the resolving power to discriminate between a solution of rod-like particles and a highly polydisperse system.

The effective diffusion coefficients presented above resulted from the average effect of all the species in the solution without taking into account the angle dependence of the intensity of light scattered by the rod-like particles. Further investigation of the myosin system required more detailed modeling. We used the two sphere model and the two cylinder model to fit the autocorrelation function of the samples. The former took into ac-

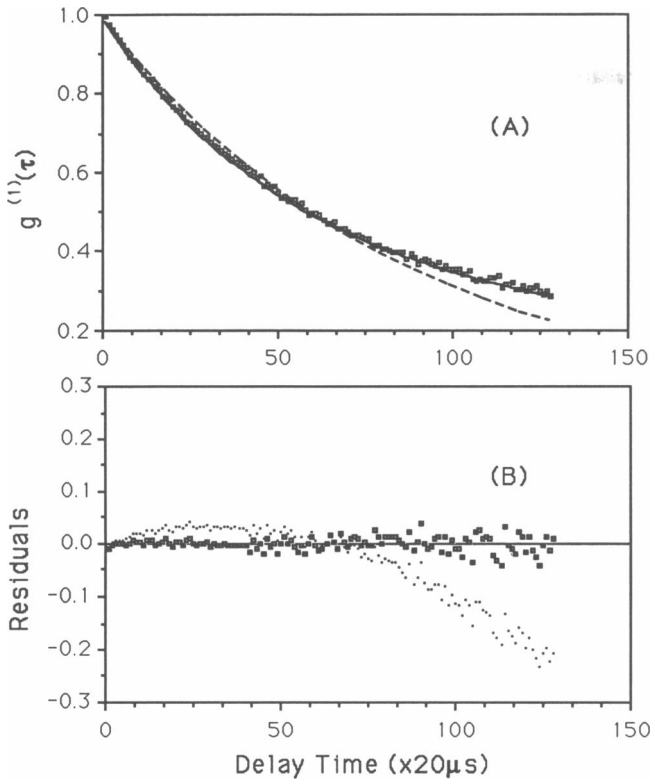

FIGURE 3 Autocorrelation function of smooth muscle myosin. Fitted curves (*A*) and residuals (*B*) of the autocorrelation function, $g^{(1)}(\tau)$, of myosin are presented as a function of delay time. The squares represent experimental data collected at 30°. The solid line corresponds to the fits of the two sphere model, and the dashed line corresponds to the fits of the cumulant method. The residuals were defined as the difference between the experimental data and fitted curves normalized by the experimental data: i.e., residuals = (theoretical value − experimental value)/experimental value.

count the polydispersity and the latter included effects due to the asymmetry of rod-like particles.

Two sphere model fitting

The two sphere model was used on the data collected at a scattering angle of 30°, where contributions from rotational diffusion of the myosin species can be neglected. Only the translational diffusion coefficient, D_t, and the weight fraction for each species were determined by the model (Eq. 7). The fitting was performed on the data collected from three preparations of unphosphorylated myosin and two preparations of phosphorylated myosin. Fig. 3 shows the typical fitted curves and the fitting residuals of the autocorrelation function $g^{(1)}(\tau)$ obtained from the two sphere model and the cumulant fitting. The two sphere model fitting is clearly superior to the cumulant fitting.

For all the samples, the weight fractions of the two species in the model exhibited little dependence on salt concentration. The major species with a fraction of 60–80% had a value of D_t, between 1.14×10^{-7} and 2.13×10^{-7} cm^2/s over KCl concentrations ranging from 0.05 to 0.5 M. This range of D_t was comparable to the expected values for the two conformational forms of monomeric myosin. However, the values of D_t for the other species were only one- to two-tenths of that for the major species (data not shown). This minor species must have been much larger than monomeric myosins, and therefore, was regarded as a large aggregate present in the solution.

The major species in both the unphosphorylated and the phosphorylated myosin, had a diffusion coefficient of $1.26 \pm 0.12 \times 10^{-7}$ cm^2/s at salt concentrations above 0.3 M KCl, and $2.07 \pm 0.06 \times 10^{-7}$ cm^2/s at salt concentrations below 0.15 M KCl. If at the high salt concentrations myosin is modeled as a rigid rod with a radius of 1 nm, the value of D_t corresponds to a myosin length of 158.0 ± 13.0 nm, which is the estimated length of the fully extended monomer. If at low salt concentrations the rod radius is assumed to be 3 nm, then the value of D_t corresponds to a myosin length of 38.5 ± 2.5 nm, or slightly less than one-third the length of the fully extended form. Fig. 4 shows that changes in the diffusion coefficient D_t of the major species depended on the phosphorylation of the myosin light chain in the intermediate range of salt concentration from 0.15 to 0.3 M KCl. It supports the conclusion that the phosphorylated myosin unfolds from its compact form at a lower ionic strength than unphosphorylated myosin.

The presence of a slowly diffusing species other than the two monomeric forms found by the two sphere model fitting suggests that the two myosin monomeric

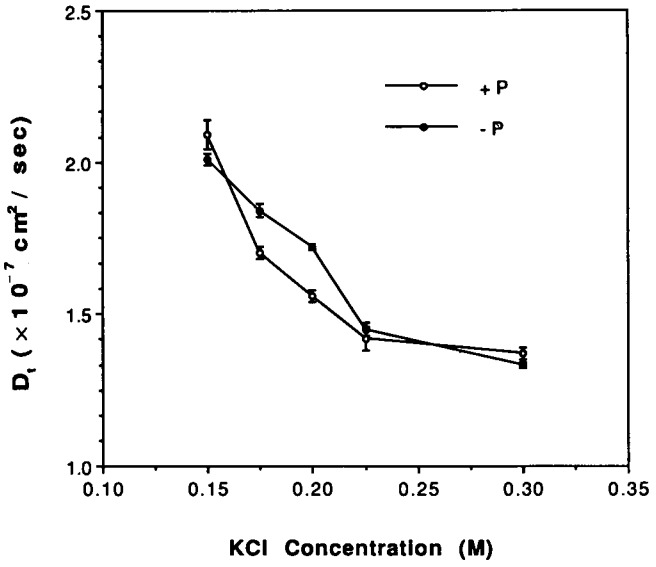

FIGURE 4 Translational diffusion coefficient, D_t, of unphosphorylated (●) and phosphorylated (○) myosin as a function of KCl concentration. Each value of D_t corresponds to the major species that resulted from the fits of the two sphere model at a scattering angle of 30°. The experimental conditions were the same as those in Fig. 2.

forms coexist with polymeric forms in solution. This might have been the reason for the high polydispersity at 30° found by the cumulant fit. Due to lack of a priori knowledge about the large species, we could not estimate its shape and dimensions, making it difficult to give a more quantitative description of the system. However, because the contribution to the scattered light from large species decreases with increasing scattering angle, it is possible to characterize the transition between the two monomeric forms more precisely at a larger scattering angle.

Two cylinder model fitting

The two cylinder model was applied to the data collected at a scattering angle of 90°. Since the rotational diffusion of the myosin molecule could not be neglected under this condition, this model took some account of the asymmetry of the species. The scattered optical field contained components that arise from rotational and translational diffusion. The extended and folded forms of monomeric myosin were assumed to be two different thin rigid cylinders of length L for which $qL \leq 10$. Their autocorrelation function was described by Eq. 10. We first specified the size of one species, the folded myosin, and varied the size for the other species about the size expected for the extended myosin. The fitting was also performed by specifying the size of the extended form and varying the size of the second species about that of the folded form. However, excessively large fitting errors were found in most instances, indicating that the system must have contained significant amounts of a third species other than the extended or folded forms.

To separate the folded form from the other species, we specified a size for the folded myosin and put no constraints on the other species. The fitting errors, measured by χ_ν^2 were close to unity in most of the cases under this condition. Fig. 5 presents the weight fraction for the folded form of myosin as a function of salt concentration obtained at 90° scattering angle. In the model, the size of the folded form was specified as having a length of 50 nm and a radius of 3 nm. The weight fraction for the phosphorylated folded form decreased at a lower ionic strength than that for the unphosphorylated folded form in the range of 0.15 to 0.3 M KCl, as shown in Fig. 5. This result clearly shows that phosphorylation promotes smooth muscle myosin unfolding, which agrees with the result of the two sphere model fitting. The folded myosin made up 60–80% of the total mass of the species in solution at low salt concentration (KCl ≤ 0.15 M), and 30–40% at high salt concentration (KCl > 0.4 M). The third species appeared in irregular sizes, varying from 145 to 400 nm in length and 1 to 20 nm in radius, depending on the salt concentration. This result can be explained by postulating the existence of polymeric forms of myosin in solution. This polymeric species might be a mixture of the extended monomeric form with polymers of the extended form. We could not resolve the composition of this irregular large species using the two species model.

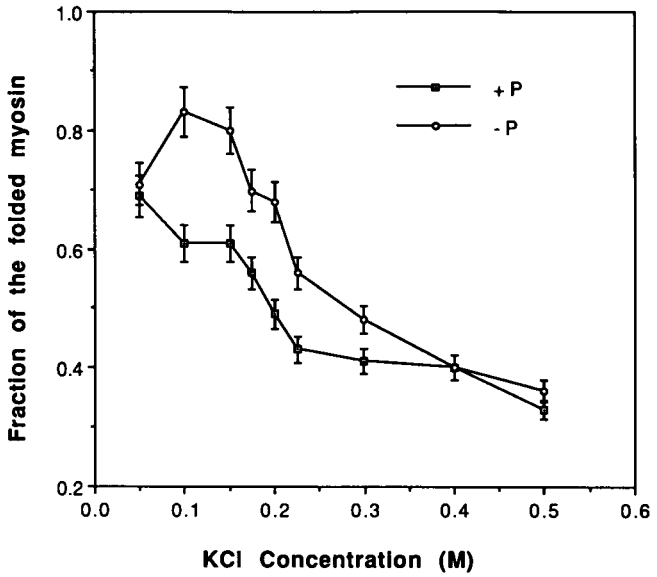

FIGURE 5 Fraction of the folded myosin obtained using the two cylinder model at 90° scattering angle as a function of KCl concentration. The circles represent the unphosphorylated myosin and the squares represent the phosphorylated myosin. The experimental conditions were the same as those in Fig. 2.

CONCLUSION AND DISCUSSION

Conformational transition of myosin monomer

Smooth muscle myosin from turkey gizzard has been shown by quasi-elastic light scattering to have two different monomeric conformations, the folded and the extended forms. These two forms have the light scattering properties of the 6S and 10S forms found in sedimentation velocity, viscometry, and electron microscopy studies (Onishi and Wakabayashi, 1982; Trybus et al., 1982). The transition between these two forms is dependent on the salt concentration and occurs between 0.15 to 0.3 M KCl where light chain phosphorylation promotes unfolding of the myosin. This observation agrees with the results obtained by sedimentation velocity studies (Trybus and Lowey, 1984).

Flexibility

The shape of the myosin molecule was assumed to be a rigid rod for each of the two forms considered in the two sphere and two cylinder models. This assumption was made without considering the effects caused by motion of the myosin heads and possible bending within the rod over the duration of measurements. The internal motions of myosin can result in a coupling between translational and rotational diffusive motions of the whole mol-

ecule. It is known that the translational and rotational diffusion is insensitive to the motion of the flexible region between the heads and rod of skeletal myosin (Garcia de la Torre and Bloomfield, 1980). Since smooth muscle myosin has a structure similar to skeletal myosin, we have ignored possible hydrodynamic effects of the heads and consider only contributions arising from possible changes in bending of the smooth muscle myosin rod.

Bending about a hinge within a rod causes an increase in the translational diffusion (Harvey, 1979). A theoretical treatment of translational-rotational coupling in diffusion, from the viewpoint of QELS, has been developed by Fujime and co-workers (Fujime and Maruyama, 1973, Maeda and Fujime, 1981, Maeda and Fujime, 1984). The evaluation of the effect of change in flexibility over time on $g^{(1)}(\tau)$ requires extensive numerical calculations. However, a semi-quantitative assessment can be obtained by comparing the observed value of the decay rate, $\bar{\Gamma}$, with the theoretically calculated value for a given rod in the cumulant analysis. If the observed value of $\bar{\Gamma}$ exceeds the theoretical value, a contribution from coupling due to changing filament flexibility over time should be considered (Maeda and Fujime, 1984). No sign of coupling was observed for the two myosin species examined at the extremes of the salt concentrations (KCl < 0.1 M or KCl > 0.3 M). All the values of $\bar{\Gamma}$ obtained at high salt concentrations were not greater than the expected value for the extended monomeric myosin model. The same was true for the folded monomeric myosin model at low salt concentrations. In conclusion, no detectable flexible motions were observed, giving support to the rigid rod assumption for the smooth muscle myosin molecule under these conditions.

In the transition phase (0.15 M < KCl < 0.3 M) where myosin undergoes a shape change, $\bar{\Gamma}$ increased from the value taken at the high salt solution to the value at the low salt solution. It was unlikely that myosin molecules uniformly bend into an intermediate form at a KCl concentration within the transition range, because the value of the polydispersity index, Q, would have been much smaller than the observed values (~0.4). The myosin solution might have contained either a mixture of intermediates or have had different fractions of the extended and folded forms, as assumed in the two species model. However, investigation of these two possibilities was excluded by the limited accuracy of our data analysis methods and the presence of myosin aggregates.

Interaction of smooth muscle myosin

Another assumption used in the QELS data analysis was that the sample solution is infinitely dilute in order to exclude any significant interaction between species. Molecular interactions (excluded volume effects, electrical charge effects, and other interactions causing mutual repulsion of the particles) can cause an increase in the effective diffusion coefficient (Pusey and Tough, 1985). The noninteraction condition can be met by working with dilute solutions, where the volume swept out by the rotation of a rod-like particle about its center is much larger than the average volume of a single particle. The dilute concentration regimes of the monomeric myosins are below 0.25 mg/ml for an extended form (L = 150 nm) and 6.75 mg/ml for a folded form (L = 50 nm). All myosin samples measured by QELS had concentrations below 0.15 mg/ml, which was well within the dilute regimes for monomeric myosin. There was no significant discrepancy between the observed and the calculated values of $\overline{D_{\text{eff}}}$ for the extended and folded forms of the myosin in the cumulant analysis. Interparticle interactions were negligible, although aggregates may have existed in solution.

A multi-component system

Our results show that smooth muscle myosin solutions contain not only the two monomers but larger particles, possibly filaments for [KCl] range from 0.05 to 0.5 M. It is unlikely that the third filamentous species was due to an irreversibly aggregated or denatured protein, because preparations were taken from the center of the monomer peak following column purification; any irreversibly aggregated or denatured protein should have been removed. After the column purified sample was dialyzed to the desired salt concentration, the sample was further clarified by high speed centrifugation (100,000 g) and filtration. Impurities and dust should have been minimized following these procedures. No significant difference in sample polydispersity was observed when two subsequent measurements were made on the same sample before and after being spun at the low speed (1,000 g), and after storage at 4°C overnight. The polydispersity index, Q, is both a measure of the polydispersity of a solution as well as the asymmetry of the particle contained in the solution. If the system contains only a folded and an extended monomeric species, the theoretical estimation of Q is 0.02 to 0.19 depending on the scattering angle. However, much higher values of Q (0.12–0.6) were obtained from the cumulant analysis, which suggests a highly polydisperse myosin solution containing large particles. When the data was further analyzed using the two sphere model and the two cylinder model, a slowly diffusing species, together with the two monomeric forms, was observed over the salt concentration range from 0.05 to 0.5 M KCl for the phosphorylated and unphosphorylated myosin. Since the possibility that the preparation contained a large amount of impurity was excluded, this slowly diffusing species is believed to result from an equilibrium between polymers and monomers of smooth muscle myosin. However, the two species models assume that there are no filamentous species present, and therefore, they could only separate the predominant monomeric myosin species from the remaining components contained in the system. The as-

signed weight fraction and size of the slowly diffusing species were actually due to a combined effect of the polymeric forms and the minor monomeric form. The size, composition, and change in the fraction of the possible polymeric forms could not be resolved. We were unable to observe a clear shift of the equilibrium between polymeric forms and the monomeric forms with ionic strength, because the two species models lack the required resolving power.

The dimensions of the slowly diffusing species observed with the two species model appeared to be different at the different salt concentration and phosphorylation conditions. The configuration and composition of the polymers might vary with changes in ionic conditions and phosphorylation. Different intermediates assembled from the myosin monomers might also exist in solution and form filaments. Such effects could have resulted in the different sizes of the slowly diffusing species observed in data analysis at various ionic strengths.

Fig. 5 clearly shows the transition of the myosin monomer unfolding. However, the observed weight fraction of the folded monomer was higher than the results obtained by gel filtration, electron microscopy, and sedimentation velocity at the high salt concentration (KCl > 0.4 M). This difference may be attributed to the fact that the system is not under equilibrium conditions when measured by these methods. Also, the presence of polymeric species in solution might have caused a bias in the fitting parameters of our models. As suggested by the higher values of the polydispersity index in high salt concentrations, more polymeric forms were present in high salt concentration than in low salt concentration. It is possible that the higher fraction of the folded form obtained from the two cylinder model analysis has a greater error due to greater variability in filament assembly in the high salt solution.

Below 0.1 M KCl, the folded monomer has been shown to form an antiparallel folded dimer that sediments at 15S (Trybus and Lowey, 1984). Two-thirds of the antiparallel folded dimer and one-third of the folded monomer were observed at 0.05 M KCl using electron microscopy. However, our fitting error became excessively large when the folded dimer and the folded monomer were assumed to be the two species in the models at KCl concentration below 0.1 M. This indicates that the folded dimer was not a major component in the solution. The predominant component was found to be the folded monomer and the remaining component was much longer than the folded dimer at KCl concentration below 0.1 M. The discrepancy between our observation and that of electron microscopy could be due to perturbations in the equilibrium of the myosin molecules induced by changing salt concentration and adding glycerol during specimen preparation for electron microscopy. It is possible, however, that the antiparallel folded dimer existed in the solution as a part of the remaining component which we were unable to identify.

In conclusion, our observations support the coexistence of polymeric myosin with two configurations of monomeric myosin under equilibrium conditions. This in turn supports the hypothesis of a dynamic equilibrium in solution between the two monomers and filaments (Kendrick-Jones et al., 1987). To further understand the equilibrium process in solution, the polymeric forms must be characterized with respect to their shape and size. A multi-species model is needed for a better description of the system. Currently, procedures for analyzing the QELS spectra of such models do not exist.

We thank Dr. James Sellers of the National Institutes of Health for providing phosphorylated smooth muscle myosin.

This work was supported by USPHS NIAMSD grant AR12803 to F. D. Carlson.

Received for publication 1 July 1991 and in final form 24 February 1992.

REFERENCES

Ankrett, R. J., A. J. Rowe, R. A. Cross, J. Kendrick-Jones, and C. R. Bagshaw. 1991. A folded (10S) conformer of myosin from a striated muscle and its implications for regulation of ATPase activity. *J. Mol. Biol.* 217:323–335.

Bevington, P. R. 1969. Data Reduction and Error Analysis for the Physical Sciences. McGraw-Hill, Inc., New York. 336 pp.

Broersma, S. 1960a. Rotational diffusion constant of a cylindrical particle. *J. Chem. Phys.* 32:1626–1631.

Broersma, S. 1960b. Viscous force constant for a closed cylinder. *J. Chem. Phys.* 32:1632–1635.

Broersma, S. 1981. Viscous force and torque constants for a cylinder. *J. Chem. Phys.* 74:6989–6990.

Chu, B. Esin Gulari, and Erdogan Gulari. 1979. Dynamics of macromolecular solutions. *Phys. Scripta.* 19:467–485.

Craig, R., R. Smith, and J. Kendrick-Jones. 1983. Light-chain phosphorylation controls the conformation of vertebrate non-muscle and smooth muscle myosin molecules. *Nature (Lond.).* 302:436–439.

Cross, R. A., A. P. Jackson, S. Citi, J. Kendrick-Jones, and S. R. Bagshaw. 1988. Active site trapping of nucleotide by smooth and non-muscle myosins. *J. Mol. Biol.* 203:173–181.

Cummins, H. Z. 1982. Analysis of diffusion of biological materials by quasielastic light scattering. *In* The Application of Laser Light Scattering to the Study of Biological Motion. J. C. Earnshaw and M. W. Steer, editors. Plenum Press, New York and London. 171–208.

Dahneke, B. E. 1983. Measurement of Suspended Particles by Quasi-Elastic Light Scattering. John Wiley & Sons, Inc., New York. 570 pp.

Fujime, S., and M. Maruyama. 1973. Spectrum of light quasielastically scattered from linear macromolecules. *Macromolecules.* 6:237–241.

Garcia de la Torre, J. and V. A. Bloomfield. 1980. The conformation of myosin in dilute solution as estimated from hydrodynamic properties. *Biochemistry.* 19(22):5118–5123.

Harvey, S. C. 1979. Transport properties of particles with segmental flexibility I. hydrodynamic resistance and diffusion-coefficients of a freely hinged particle. *Biopolymers.* 18:1081–1104.

Kendrick-Jones, J., R. C. Smith, R. Craig, and S. Citi. 1987. Polymerization of vertebrate non-muscle and smooth muscle myosins. *J. Mol. Biol.* 198:241–252.

Kerker, M. 1969. The Scattering of Light and Other Electromagnetic Radiation. Academic Press, New York. 666 pp.

Koppel, D. E. 1972. Analysis of macromolecular polydispersity in intensity correlation spectroscopy: the method of cumulants. *J. Chem. Phys.* 57(11):4814–4820.

Levenberg, K. 1944. A method for the solution of certain non-linear problems in least squares. *Quart. Appl. Math.* 2:164.

Mandel, L. 1963. Fluctuations of light beams. *Prog. Opt.* 2:183.

Marquardt, D. W. 1963. An algorithm for least-squares estimation of nonlinear parameters. *J. Soc. Ind. Appl. Math.* 11:431.

Maeda, T., and S. Fujime. 1981. Effect of filament flexibility on the dynamic light-scattering spectrum with special reference to fd virus and muscle thin filaments. *Macromolecules.* 14:809–818.

Maeda, T., and S. Fujime. 1984. Spectrum of light quasielastically scattered from solutions of very long rods at dilute and semi-dilute regimes. *Macromolecules.* 17:1157–1167.

Montague, C., and F. D. Carlson. 1982. Preparation of contractile proteins for photon correlation spectroscopes and classical light-scattering studies. *Methods Enzymol.* 85:562–570.

Newman, J., and F. D. Carlson. 1980. Dynamic light scattering evidence for the flexibility of native muscle thin filaments. *Biophys. J.* 29:37–47.

Oliver, C. J. 1974. Correlation techniques. *In* Photon Correlation Light Beating Spectroscopy. H. Z. Cummins, editor. Plenum Press, New York. 151–224.

Onishi, H., and J. Wakabayashi. 1982. Electron microscopic studies of myosin molecules from chicken gizzard muscle. I. Formation of the intramolecular loop in the myosin tail. *J. Biochem. (Tokyo).* 92:871–879.

Pecora, R. 1985. Dynamic Light Scattering. Plenum Press, New York. 420 pp.

Provencher, S. W. 1976a. A Fourier method for the analysis of exponential decay curves. *Biophys. J.* 16:27–41.

Provencher, S. W. 1976b. An eigenfunction expansion method for the analysis of exponential decay curves. *J. Chem. Phys.* 64:2772–2777.

Provencher, S. W., J. Hendrix, and L. De Maeyer. 1978. Direct determination of molecular weight distributions of polystyrene in cyclohexane with photon correlation spectroscopy. *J. Chem. Phys.* 69:4273–4276.

Provencher, S. W. 1979. Inverse problems in polymer characterization direct analysis of polydispersity with photon correlation spectroscopy. *Markromol. Chem.* 180:201–209.

Pusey, P. N., and R. J. A. Tough. 1985. Particle interactions. *In* Dynamic Light Scattering. R. Pecora, editor Plenum Press, New York. 85–171.

Sellers, J. R., M. D. Pato, and R. S. Adelstein. 1981. Reversible phosphorylation of smooth muscle myosin, heavy meromyosin, and platelet myosin. *J. Biol. Chem.* 256(24):13137–13142.

Suzuki, H., H. Onishi, K. Takahashi, and S. Watanabe. 1978. Structure and function of chicken gizzard myosin. *J. Biochem. (Tokyo).* 84:1529–1542.

Trybus, K. M., T. W. Huiatt, and S. Lowey. 1982. A bent monomeric conformation of myosin from smooth muscle. *Proc. Natl. Acad. Sci. USA.* 79:6151–6155.

Trybus, K. M., and S. Lowey. 1984. Conformational states of smooth muscle myosin. *J. Biol. Chem.* 259(13):8564–8571.